Appl. Phys. A 79, 697–700 (2004)
DOI: 10.1007/s00339-003-2252-z

Applied Physics A
Materials Science & Processing

S.C. LYU[1]
H.W. KIM[2]
S.J. KIM[3]
J.W. PARK[4]
C.J. LEE[1,✉]

Synthesis and crystallinity of carbon nanotubes produced by a vapor-phase growth method

[1] Department of Nanotechnology, Hanyang University, Seoul 133-791, Korea
[2] School of Materials Science and Engineering, Inha University, Incheon 402-751, Korea
[3] School of Electrical and Electronic Engineering, Kyungnam University, Masan 631-701, Korea
[4] School of Advanced Materials Science Engineering, Hanyang University, Seoul 133-791, Korea

Received: 10 March 2003/Accepted: 2 June 2003
Published online: 25 July 2003 •

ABSTRACT We have studied the effect of temperature on the growth and crystallinity of carbon nanotubes (CNTs), synthesized by a vapor-phase growth method using a catalytic reaction of iron pentacarbonyl ($Fe(CO)_5$) and acetylene (C_2H_2) gas. By increasing the growth temperature from 750 °C to 950 °C, both the growth rate and the diameter of the CNTs increase. Moreover, the crystallinity of the graphite sheets improves progressively with increasing growth temperature. Adjustment of the growth temperature gives potential for controlled growth of CNTs in a large-scale synthesis of CNTs.

PACS 61.46.+w; 68.37.-d; 81.07.De

1 Introduction

Since the first discovery of carbon nanotubes (CNTs) in 1991 [1], CNTs have attracted much attention because of many potential applications in field emission displays (FEDs) [2], as tips for scanning probe microscopy [3], hydrogen storage [4], chemical sensors [5] and high-strength composites [6].

For the production of CNTs, various synthetic methods such as arc-discharge [7, 8], laser vaporization [9], pyrolysis [10], plasma-enhanced chemical vapor deposition (CVD) [11, 12], thermal CVD [13, 14] and vapor-phase growth [15–20] have been developed. Among the various growth techniques, the vapor-phase growth method especially has the advantage of mass production of CNTs. In the vapor-phase growth method, the growth temperature is one of the crucial parameters for the growth rate and the crystallinity of the CNTs. There are some reports about the temperature effect on the CNTs synthesized by CVD on silicon or silicon oxide substrates. Lee et al., using thermal CVD, reported that the growth rate, diameter and crystallinity of CNTs were effectively controlled by the growth temperature [21]. Li et al. also showed that the growth and the structure of CNTs are strongly affected by the growth temperature [22]. Recently, using Raman spectroscopy, Nerushev et al. revealed that the crystallinity of CNTs produced by thermal CVD was improved by increasing the growth temperature [23]. In previous work, we reported that the growth rate and the crystallinity of CNTs could be adjusted by an Ar flow rate and an C_2H_2 direct bubbling process [24]. But there were few reports on the systematic study of temperature effects on the growth and the crystallinity of CNTs synthesized by the vapor-phase growth method.

In this paper, we report the effect of temperature on the growth and the crystallinity of CNTs produced by the vapor-phase growth method using a simple catalytic reaction of the mixture of $Fe(CO)_5$ and C_2H_2 gases. Scanning electron microscopy (SEM) was used to measure the length and the diameter of the CNTs and transmission electron microscopy (TEM) was used to evaluate the structure and the crystallinity of the CNTs. In order to obtain overall information on the crystallinity of specimen, we investigated thermo-gravimetric analysis (TGA) and Raman spectroscopy of CNTs.

2 Experimental

The vapor-phase growth system is described elsewhere [24]. In order to synthesize CNTs, C_2H_2 gas was directly bubbled through a liquid $Fe(CO)_5$ source maintained at room temperature, and Ar gas was used as a carrier gas. All the gases were directly introduced into a reactor, consisting of a horizontal quartz tube with an inner diameter of 20 mm and a heating zone of 200 mm. Ar carrier gas of 500 sccm was flowed into the reactor while arriving at the preset temperature. The CNTs was synthesized by supplying C_2H_2 and Ar carrier gases with flow rates of 20 sccm and 1500 sccm, respectively, in the temperature range 750–950 °C for 30 min. After the reaction, 500 sccm of Ar gas was flowed into the reactor while cooling to room temperature.

An SEM (Hitachi S-800, 30 kV) was used to measure the length and diameter of the CNTs. We measured both the length and the diameter of CNTs using SEM images, and calculated the average value of those CNT parameters from eight experimental runs.

An TEM (Philips, CM20T, 200 kV) was used to investigate the structure and the crystallinity of the CNTs. The deposits were separated from the quartz tube and then dispersed on a carbon TEM microgrid. Thermo-gravimetric analysis

✉ Fax: +82-2/2290-0768, E-mail: cjlee@hanyang.ac.kr

(TGA) (SDT 2960, TA instrument) and Raman spectrometry (Renishaw micro-Raman 2000) were used to evaluate the overall crystallinity of the CNTs. An TGA was used for temperature-programmed oxidation at a constant heating rate of 10 °C/min in ambient air. The weight loss of the CNTs was recorded as a function of temperature and time. For Raman analysis, the 632.8-nm line of a He-Ne laser was used for excitation.

3 Results and discussion

Figure 1 shows the SEM micrographs of carbon materials synthesized at 750–950 °C. Large amounts of carbon deposits were produced using the $Fe(CO)_5$-C_2H_2 system and the products were densely packed and accumulated on the surface of quartz tube inside. The products were homogeneously deposited everywhere on the inner surface of the reactor regardless of the position inside the reactor. In our experiments, we used a high Ar flow rate to obtain a uniform distribution of catalyst within the quartz tube [17, 25].

Magnified SEM images show that the carbon deposits were of high-purity CNTs without carbonaceous particles on the surface. From SEM observation, the lengths of CNTs were in the range 130–142, 200–240, and 260–290 μm at the growth temperature of 750, 850, and 950 °C, respectively. After several experiments, we calculated that the average lengths of CNTs were 140, 220, and 280 μm, respectively, at the growth temperatures of 750, 850, and 950 °C. The length of the CNTs, which is proportional to the productivity of the carbon deposits, was increased by increasing the growth temperature. This result is probably caused by enhanced diffusion and reaction rates of carbon within Fe catalyst particles. Further study is necessary to obtain quantitative kinetic information. In this work, the diameter distribution of the CNTs was in the range of 20–30, 28-38, and 36–50 nm at the growth temperature of 750, 850, and 950 °C, respectively. We also calculated average diameters of the CNTs to be 25, 34, and 40 nm, at the growth temperature of 750, 850, and 950 °C, respectively. The diameter of the CNTs increases due to the size increase of catalyst particles with increasing the growth temperature. The catalyst particles have a larger diameter and a broad size distribution because more significant agglomeration occurs at higher growth temperatures.

Figure 2a, b and c shows low-magnification TEM images of CNTs grown at 750, 850, and 950 °C, respectively. The CNTs have a multiwalled structure with a hollow inside and have no carbonaceous particles on the surface. To investigate an effect of the growth temperature on the crystallinity of graphite sheets, high-resolution TEM (HRTEM) images of CNTs were investigated. Figure 2d, e and f shows typical HRTEM images of CNTs grown at 750, 850, and 950 °C, respectively. The HRTEM image of a CNT grown at 750 °C shows the waving structure of graphitic sheets at a short range, as shown in Fig. 2d. It is well known that the waving structure is caused by a defective structure in the graphite sheet. In this experiment, the defective graphite sheets result from insufficient reaction energy. The HRTEM image of a CNT grown at 850 °C reveals a more crystalline structure compared with CNTs grown at 750 °C, as shown in Fig. 2e. The HRTEM image of a CNT grown at 950 °C shows well-ordered and straight lattice fringes, as shown in Fig. 2f. The crystallinity of the graphite sheets improves at higher growth temperatures. However, the surface walls of the nanotubes, which correspond to the outer graphite sheets, have incoherent crystal structures due to defective carbon network formation.

The temperature-programmed oxidation technique is a useful method for investigating the overall crystallinity of CNTs. Figure 3 is a plot of weight loss in percentage vs oxidation temperature, measured by heating the CNTs in a TGA. The percentage-weight-loss curve between 200 °C and 800 °C is plotted by adjusting to 100% the weight loss

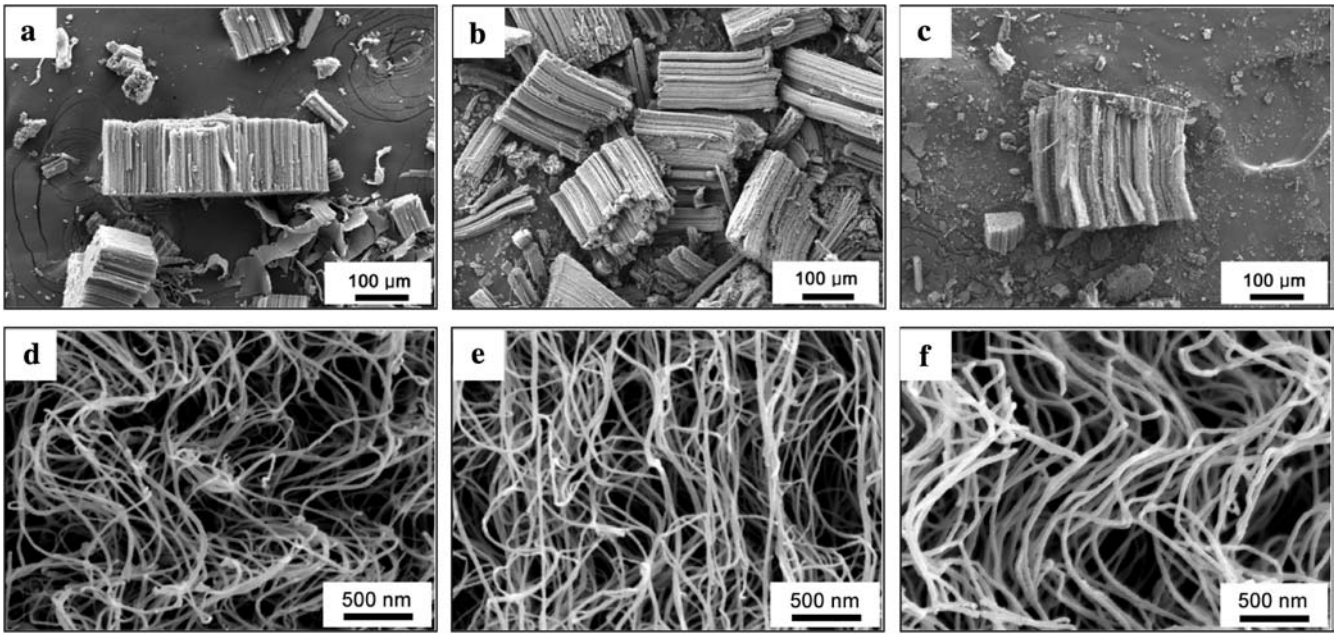

FIGURE 1 SEM images of CNTs synthesized at 750–950 °C for 30 min. SEM image of CNTs grown at 750 °C (**a**, **d**); 850 °C (**b**, **e**); and 950 °C (**c**, **f**)

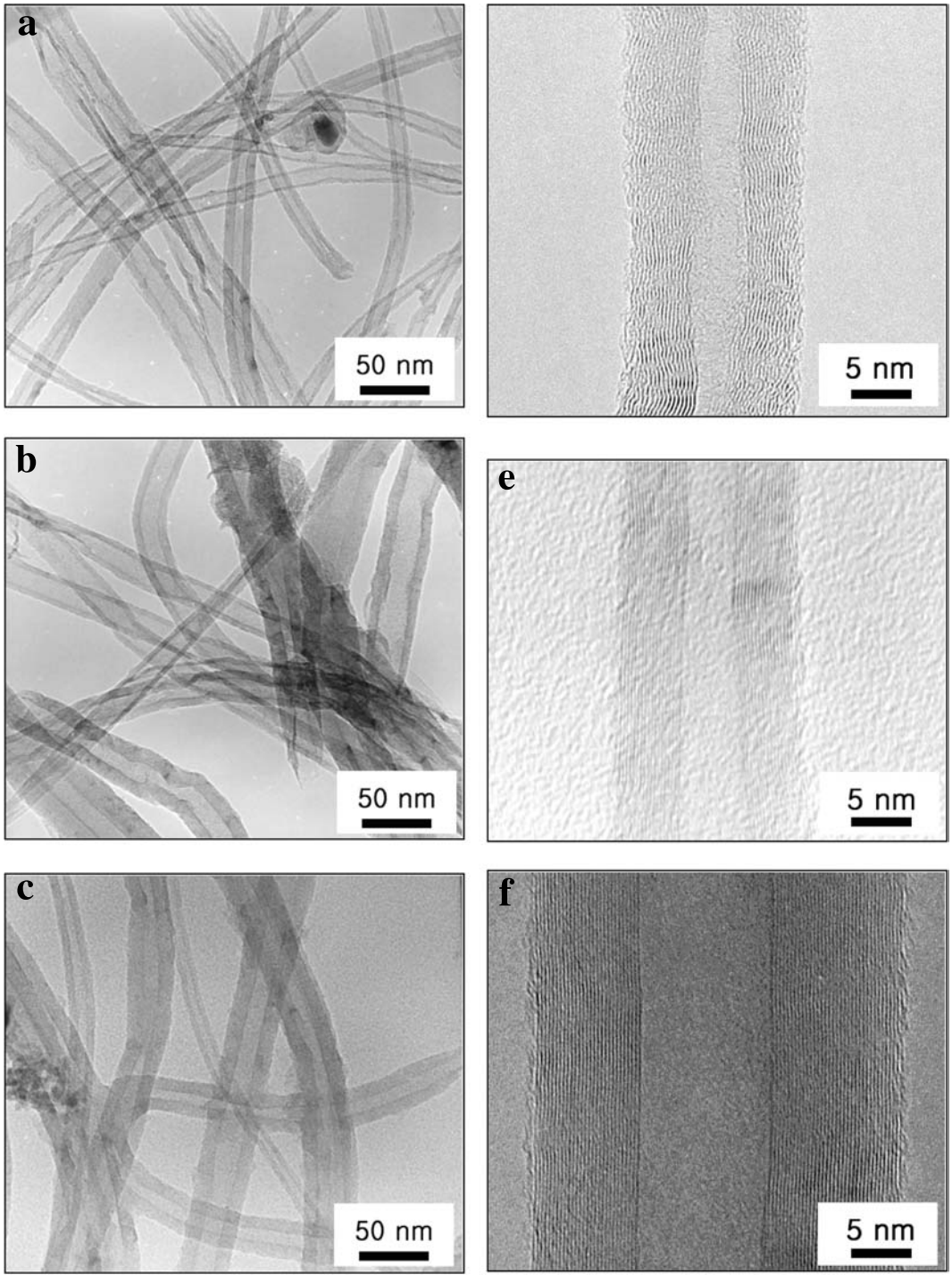

FIGURE 2 TEM images of the CNTs **a**, **b** and **c** at low magnification and **d**, **e** and **f** at high magnification, grown at different temperatures: 750 °C (**g**, **d**); 850 °C (**b**, **e**); and 950 °C (**c**, **e**)

of CNTs excluding the catalyst. In this work, we evaluated the weight of residual catalyst for each growth temperature after burning the CNTs perfectly at 800 °C, which was less than about 10% of the product weight of CNTs. For the CNTs synthesized at each growth temperature, an TGA measurement was conducted separately. Figure 3 shows that the gasification of CNTs grown at 750, 850, and 950 °C starts at approximately 370, 460, and 490 °C, respectively. This result indicates that the overall crystallinity of CNTs improves by increasing the growth temperature, which is consistent with the TEM analysis.

Figure 4 shows the first-order Raman spectra of the as-grown CNTs. The Raman spectra show two main bands at approximately 1335 cm^{-1} (D-band) and approximately 1580 cm^{-1} (G-band), which indicates multiwalled CNTs. The G-band reveals a typical graphite structure, but the D-band indicates the defective feature of graphite sheets [26]. The peak intensity ratio of D- and G-bands decreases with in-

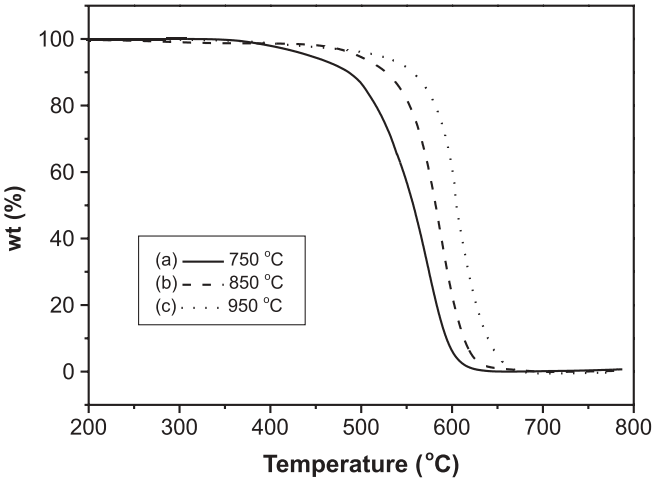

FIGURE 3 TGA data of weight loss in percentage vs oxidation temperature for the CNTs grown at: **a** 750 °C; **b** 850 °C; and **c** 950 °C

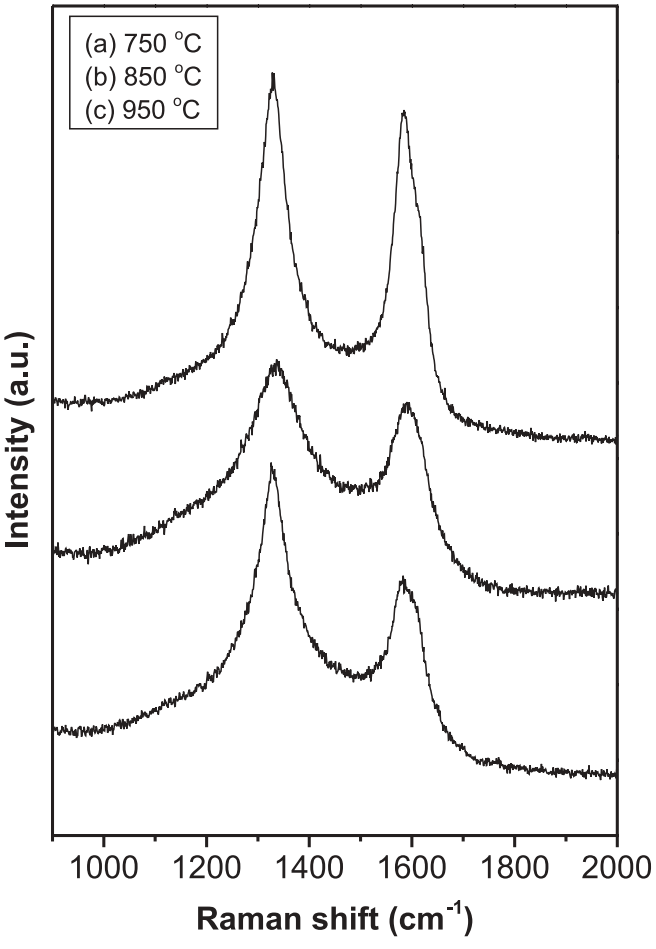

FIGURE 4 Raman spectra of CNTs grown at: **a** 750 °C; **b** 850 °C; and **c** 950 °C. The peak intensity ratio of D- and G-bands decreases with increasing the growth temperature

creasing the growth temperature. This result means that the crystallinity of the graphite sheets increases at higher growth temperatures.

4 Summary

We have investigated the effect of temperature on the growth and the crystallinity of CNTs using a catalytic reaction of a C_2H_2 and $Fe(CO)_5$ mixture at 750–950 °C. The growth rate, the diameter and the crystallinity of the CNTs increase with increasing the growth temperature. Especially, the crystallinity of CNTs is largely dependent on the growth temperature during vapor-phase growth. It is suggested that the growth rate, the diameter and the crystallinity of CNTs grown by a vapor-phase growth method can be easily controlled by growth temperature.

ACKNOWLEDGEMENTS This work was supported by The Center for Nanotubes and Nanostructured Composites and The National R&D Project for Nanoscience and Technology of MOST.

REFERENCES

1 S. Iijima: Nature **354**, 56 (1991)
2 W. A de Heer, A. Chatelain, D. Ugarte: Science **270**, 1179 (1995)
3 H. Dai, J.H. Hafner, A.G. Rinzler, D.T. Colbert, R.E. Smalley: Nature **384**, 147 (1996)
4 C. Liu, Y.Y. Fan, M. Liu, H.T. Cong, H.M. Cheng, M.S. Dresselhaus: Science **286**, 1127 (1999)
5 J. Kong, N.R. Franklin, C. Zhou, M.G. Chapline, S. Peng, K. Cho: Science **287**, 622 (2000)
6 P.M. Ajayan, L.S. Schadler, C. Giannaris, A. Rubido: Adv. Mater. **12**, 750 (2000)
7 S. Iijima, T. Ichihashi: Nature **363**, 603 (1993)
8 C. Journet, W.K. Maser, P. Bernier, A. Loiseau, M. Lamy de la Chapelle, S. Lefrant: Nature **388**, 756 (1997)
9 A. Thess, R. Lee, P. Nikolaev, H. Dai, P. Petit, J. Robert, C. Xu, Y.H. Lee, S.G. Kim, D.T. Colbert, G. Scuseria, D. Tomanek, J.E. fisher, R.E. Smalley: Science **273**, 483 (1996)
10 M. Terrones, N. Grobert, J. Olivares, J.P. Zhang, H. Terrones, K. Kordatos, W.K. Hsu, J.P. Hare, P.D. Townsend, K. Prassides, A.K. Cheetham, H.W. Kroto, D.R.M. Walton: Nature **388**, 52 (1997)
11 Z.F. Ren, Z.P. Huang, J.W. Xu, J.H. Wang, P. Bush, M.P. Siegal, P.N. Provencio: Science **282**, 1105 (1998)
12 L.C. Qin, D. Zhou, A.R. Krauss, D.M. Gruen: Appl. Phys. Lett. **72**, 3437 (1998)
13 S. Fan, M.G. Chapline, N.R. Franklin, T.W. Tombler, A.M. Cassell, H. Dai: Science **283**, 512 (1999)
14 C.J. Lee, D.W. Kim, T.J. Lee, Y.C. Choi, Y.S. Park, Y.H. Lee, W.B. Choi, N.S. Lee, G.S. Park, J.M. Kim: Chem. Phys. Lett. **312**, 461 (1999)
15 H.M. Cheng, F. Li, G. Su, H.Y. Pan, L.L. He, X. Sun, M.S. Dresselhaus: Appl. Phys. Lett. **72**, 3282 (1998)
16 H.M. Cheng, F. Li, X. Sun, S.D.M. Brown, M.A. Pimenta, A. Marucci, G. Dresselhaus, M.S. Dresselhaus: Chem. Phys. Lett. **289**, 602 (1998)
17 M. Mayne, N. Grobert, M. Terrones, R. Kamalakaran, M. Ruhle, H.W. Kroto, D.R.M. Walton: Chem. Phys. Lett. **338**, 101 (2001)
18 R. Andrews, D. Jacques, A.M. Rao, F. Derbyshire, D. Qian, X. Fan, E.C. Dickey, J. Chen: Chem. Phys. Lett. **303**, 467 (1999)
19 B.C. Satishkumar, A. Govindaraj, C.N.R. Rao: Chem. Phys. Lett. **307**, 158 (1999)
20 F. Rohmund, L.K.L. Falk, E.E.B. Campbell: Chem. Phys. Lett. **328**, 369 (2000)
21 C.J. Lee, J. Park, Y. Huh, J.Y. Lee: Chem. Phys. Lett. **343**, 33 (2001)
22 W.Z. Li, J.G. Wen, Z.F. Ren: Appl. Phys. A **74**, 397 (2002)
23 O.A. Nerushev, R.E. Morjan, D.I. Ostrovskii, M. Sveningsson, M. Jonsson, F. Rohmund, E.E.B. Campbell: Physica B **323**, 51 (2002)
24 C.J. Lee, S.C. Lyu, H.W. Kim, C.Y. Park, C.W. Yang: Chem. Phys. Lett. **359**, 109 (2002)
25 R. Kamalakaran, M. Terrones, T. Seeger, P. Kohler-Redlich, M. Rühle, Y.A. Kim, T. Hayashi, M. Endo: Appl. Phys. Lett. **77**, 3385 (2000)
26 C.J. Lee, J. Park, S.Y. Kang, J.H. Lee: Chem. Phys. Lett. **323**, 554 (2000)